error of A/g_{11}, by calculating the mean-square deviation from the average of these data on other compounds. It is, however, apparent from the data they present that A/g_{11}, varies in the 5% range from compound to compound, and that this deviation is larger than the errors on the individual measurements of this quantity. On this basis it appears that their error is rather optimistic.

Figure 12 shows a plot of the present measured g factor versus A for Yb^{170}, Yb^{172}, Yb^{174}, and Yb^{176} with the theoretical predictions of Nilsson and Prior. It is interesting to note that the Nilsson values are close to the measured values at $A=170$ and $A=176$ and that they predict a dip near Yb^{174}; however, it appears that this dip is actually somewhat deeper than predicted by their model.

CONCLUSION

The combination of simple spectra, high counting rates, excellent signal-to-noise ratio, and wide applica- bility are advantages of the pulsed-beam Coulomb- excitation technique. Furthermore, by using the dia- magnetic ion of ytterbium no internal-field corrections are necessary. The differential angular-distribution measurement allows a careful evaluation of possible perturbations which are capable of influencing the resultant precession. In addition, it is possible to eliminate background corrections, which can limit the accuracy of the experiments.

ACKNOWLEDGMENTS

Study of the Strongly Excited 2$^+$ and 3$^-$ States in the Fe^{54,56} and Ni^{58,60,62} Isotopes by Proton Scattering at 18.6 and 19.1 MeV*

S. F. Eccles, H. F. Lutz, and V. A. Madsen†

Lawrence Radiation Laboratory, University of California, Livermore, California

(Received 23 August 1965)

Elastic and inelastic proton-scattering angular distributions were obtained at incident proton energies of about 19 MeV from Fe^{54}, Fe^{56}, Ni^{58}, Ni^{60}, and Ni^{62}. The elastic angular distributions were fitted with the nuclear optical model and the parameters so determined were compared to ascertain systematic variations. Generally the fits are good. The parameters were also used as input for distorted-wave Born-approximation (DWBA) calculations of the inelastic scattering. Of special interest was the excitation of the collective 2$^+$ and 3$^-$ states in these nuclei. The inelastic cross sections were assumed to be a result of a direct reaction exciting collective states, and in addition for the iron isotopes, calculations were made assuming single- configuration shell-model wave functions for the first 2$^+$ excited states. Although the calculated cross section is greater in Fe^{56} than in Fe^{54}, it is still far too small to explain the large difference seen experimentally. Cross sections for collective excitations were calculated assuming the DWBA, and also using the coupled- equation method. Comparisons between the two methods are made in terms of the shapes of the angular dis- tributions as well as the magnitude of the cross sections. The forward peak is reasonably fitted in all the isotopes by both the DWBA and coupled-equations calculations, but the remainder of the angular distribu- tion is not as well reproduced. The cross section for excitation of the first 2$^+$ state in Fe^{54} is not explained adequately by either the collective or particle model calculations. The identification of the collective 3$^-$ ex- cited state in Fe^{54} could not be made unambiguously.

I. INTRODUCTION

THE elastic and inelastic scattering of charged particles from separated isotopes of Fe and Ni have previously been examined with various bombard- ing particles and energies. Some recent experimental work with protons is given in Refs. 1 through 13. The first 2$^+$ excited states of the even-even isotopes have also been studied experimentally via Coulomb excita-

---

* This work performed under the auspices of the U. S. Atomic Energy Commission.
† Summer visitor at LRL. Permanent address: Physics Depart- ment, Oregon State University, Corvallis, Oregon.
[1] W. S. Gray, R. A. Kenefick, and J. J. Kraushaar, Nucl. Phys. 67, 565 (1965).
[2] T. Stovall and N. M. Hintz, Phys. Rev. 135, B330 (1964).
[3] L. L. Lee, Jr., and J. P. Schiffer, Phys. Rev. 134, B765 (1964).
[4] H. O. Funston, N. R. Roberson, and E. Rost, Phys. Rev. 134, B117 (1964).

[5] M. P. Fricke, Argonne National Laboratory Report No. ANL-6848, 1964, p. 130 (unpublished).
[6] J. Benveniste, A. C. Mitchell, B. Buck, and C. B. Fulmer, Phys. Rev. 133, B317, B322 (1964).
[7] N. R. Roberson and H. O. Funsten, Bull. Am. Phys. Soc. 9, 93 (1964), and Oak Ridge National Laboratory Report No. ORNL-CPX-2, 1964, pp. 116, 120, 124 (unpublished).
[8] J. K. Dickens et al., Phys. Letters 6, 53 (1963).
[9] G. W. Greenlees et al., Nucl. Phys. 49, 496 (1963).
[10] D. W. Devins, H. H. Forster, and G. G. Gigas, Nucl. Phys. 35, 617 (1962).
[11] K. Matsuda, Nucl. Phys. 33, 536 (1962).
[12] S. Kobayashi, J. Phys. Soc. Japan 15, 1151 (1960).
[13] M. K. Brussel and J. H. Williams, Phys. Rev. 114, 525 (1959).

tion.[14,15] Strictly theoretical studies have also been undertaken on the interpretation of the scattering from these isotopes.[16–21]

The purpose of the work reported here[22] was to obtain simultaneously both elastic and inelastic angular distributions for the strongly excited 2^+ and 3^- states in the Fe and Ni isotopes over a wide angular range (many of the previous data are very limited in angular range). One object was to fit the elastic angular distribution data with an optical model and use the parameters so obtained in calculations of the inelastic scattering. It was also desired to study systematic changes of these parameters in going from one isotope to another. In particular, Fe^{54} and Fe^{56} have very different shell structures, Fe^{54} having two proton holes in the $1f_{7/2}$ shell and a closed $1f_{7/2}$ neutron shell, while Fe^{56} has two neutrons outside the closed $1f_{7/2}$ neutron shell. The nickel isotopes have a closed $1f_{7/2}$ proton shell with two, four, and six neutrons outside the closed neutron $1f_{7/2}$ shell. The interest here is in the differences in optical-model parameters when pairs of neutrons are added to a closed shell.

An incident proton energy of around 19 MeV was chosen for this work because it was desired to be well above the region where compound nucleus effects might be important in the scattering, and this was about the upper limit of the Livermore cyclotron energy. Only the (relatively) highly excited states (the first 2^+ and 3^-, so-called collective states) in these isotopes were studied. The 2^+ state is well separated from other levels and is easily identified. The 3^- state is usually identified unambiguously, even though other states exist nearby. Other states are also seen (see Fig. 1) but many are not completely resolved because of the inherent energy spread of the cyclotron beam. It was decided to study in detail only those states which would prove unambiguous experimentally.

The elastic scattering is analyzed with the nuclear optical model. The inelastic results are analyzed in terms of a direct-reaction theory, and two different nuclear models are used to describe the wave functions. The first assumes collective excitation and uses on one hand a distorted-wave Born-approximation (DWBA) calculation, and on the other a coupled channel calculation in which the elastic scattering is coupled to the first and second 2^+ excited states. The second model
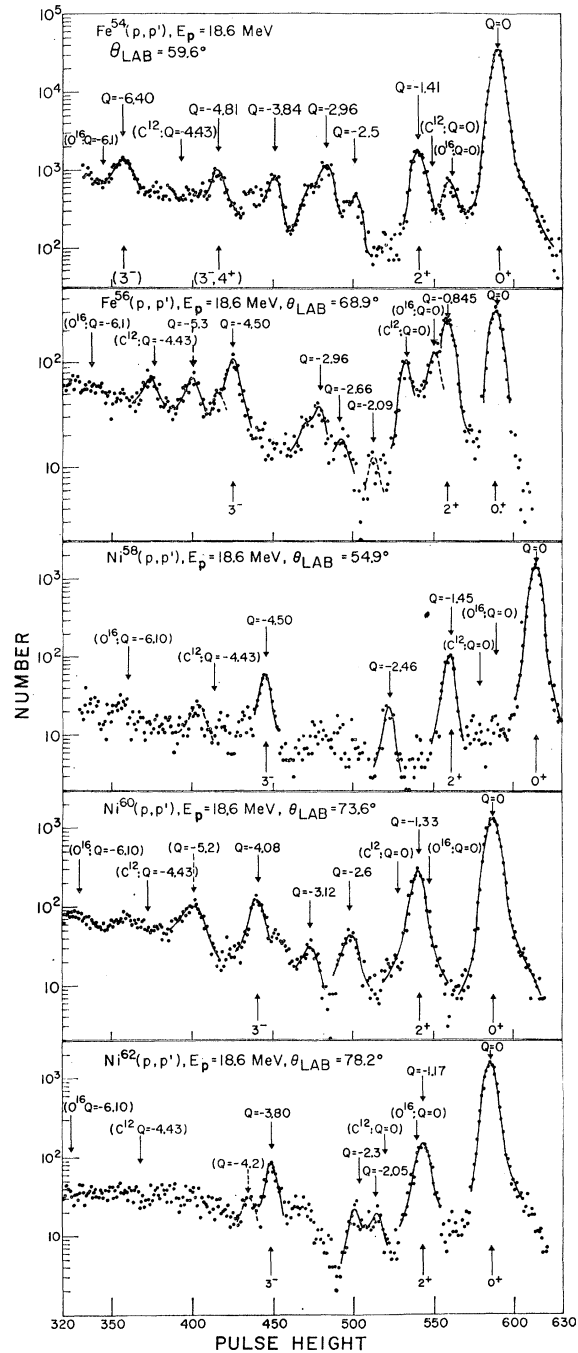
[14] J. J. Simpson, J. A. Cookson, D. Eccleshall, and M. J. L. Yates, Nucl. Phys. **62**, 385 (1965).

[15] P. H. Stelson and F. K. McGowan, Nucl. Phys. **32**, 652 (1962).

[16] V. A. Madsen and W. Tobocman, Phys. Rev. **139**, B864 (1965).

[17] R. M. Drisko, G. R. Satchler, and R. H. Bassel, Phys. Letters **5**, 347 (1963).

[18] F. G. Perey, Phys. Rev. **131**, 745 (1963).

[19] F. Perey and G. R. Satchler, Phys. Letters **5**, 212 (1963).

[20] B. Buck, Phys. Rev. **130**, 712 (1963).

[21] R. H. Bassel et al., Phys. Rev. **128**, 2693 (1962).

[22] Parts of this work have previously been reported in Bull. Am. Phys. Soc. **9**, 93 (1964); **9**, 650 (1964); **9**, 724 (1964).

FIG. 1. Typical pulse-height spectra for proton scattering from Fe^{54}, Fe^{56}, Ni^{58}, Ni^{60}, and Ni^{62}. The excited states studied in this work were the 2^+ and 3^- collective states so labeled.

assumes that the 2^+ excited state is excited by single-particle excitations rather than by a collective mode.

The experimental details and results are described and presented in Sec. II, while the theoretical models and their comparison to experiment are given in Sec. III. A discussion of these fits of theory to experi-

TABLE I. Differential cross section for $Fe^{54}(p,p')$. The cross sections are in the center-of-mass system and have units of mb/sr. $E_p = 18.6$ MeV.

$\theta_{c.m.}$ (in deg.)	$Q=0$ $d\sigma/d\Omega$	$Q=-1.41$ MeV $d\sigma/d\Omega$	$Q=-4.81$ MeV $d\sigma/d\Omega$	$Q=-6.40$ MeV $d\sigma/d\Omega$
27.4	342	3.13	...	1.1
36.9	129	3.72	...	1.2
46.4	105	2.76	0.46	1.2
51.1	87.1	2.29	0.58	0.99
55.8	56.4	1.91	0.69	0.98
60.5	29.8	1.62	0.61	0.98
65.2	11.1	1.54	...	...
74.6	6.13	1.65	0.58	0.82
79.3	11.3	1.62	0.56	0.70
84.0	15.5	1.31	0.37	0.72
93.3	14.9	1.11	0.23	0.69
102.6	7.75	0.98	0.16	0.59
111.9	3.37	1.03	0.11	0.46
116.5	2.84	0.95	...	0.50
121.2	3.03	0.74	...	0.47
125.7	3.42	0.73	...	0.50
130.3	3.90	0.69	...	0.42
135.0	4.59	0.77	...	0.54
139.5	5.09	0.79	...	0.41
144.1	5.67	0.77	...	0.35
148.8	5.63	0.85	...	0.53
157.9	5.10	0.73	...	...
±0.1	±10% absolute	±15% absolute	±25% absolute	±20% absolute

ment and the applicability of the models is given in the final section.

II. EXPERIMENTAL TECHNIQUES AND RESULTS

The Livermore variable-energy cyclotron was the source of 18.6- and 19.1-MeV protons. These energies are above the normal upper limit of the machine's operation, the higher energy being achieved by modifying the rf system and extracting the beam at a slightly larger radius. There was available roughly 10 μA of extracted beam before collimation and focusing. After bending twice, the beam was focused into a 24-in. scattering chamber and collimated to give a $\frac{1}{8}$-in. spot on the target. The nominal beam intensity at the target was 0.1 μA, and the beam was monitored by a Faraday cup-electrometer combination. The external beam, being unanalyzed, has an energy spread of about 1% at these energies, dependent on the values of the many cyclotron parameters at the time of measurement. The energy of the beam was measured by finding the range in aluminum absorbers, and the energy was held constant over the many runs to about 50 keV.

The targets were enriched isotopes from the Oak Ridge National Laboratory, the enrichment being 97% in the case of Fe^{54}, and about 99% for all the other targets. The thicknesses were nominally 1.0 mg/cm²; the actual thickness in each case was determined by either weighing or by measuring the energy loss of alpha particles from an Am^{241} source. Impurities of carbon and oxygen were noticeable in the pulse-height

spectra from the iron isotopes, but in most cases these impurities did not affect the determination of the cross sections.

Solid-state surface-barrier detectors were used to detect the scattered particles. A thin, 213-μ, ΔE detector was used to absorb the alpha particles from (p,α) reactions, and a tandem array of two 1000-μ thick detectors made up the E detector that looked at the protons. Because of the Q values for proton-induced reactions on these isotopes, only protons and low-energy deuterons appeared in the E detector. No mass identification was found to be necessary to distinguish the protons and deuterons. The spectra of alpha particles were recorded, but no results are given at this time. The signals from the detectors were sent to charge-sensitive preamplifiers and then to conventional electronics, including a linear gate which was used to eliminate many small pulses. The output of the linear gate went to a 800-channel pulse-height analyzer. The over-all energy resolution of the system, including beam spread and target thickness effects, was about 200 keV.

Typical pulse-height spectra are shown for the five isotopes in Fig. 1. On each plot each clear peak is identified by a Q value, and the position of the arrow is the calculated position of where the peak should appear, based on an energy calibration curve. Since there was contamination by carbon and oxygen, the position of the elastic and first excited states of these

TABLE II. Differential cross section for $Fe^{56}(p,p')$. The cross sections are in the center-of-mass system and have units of mb/sr. $E_p = 19.1$ MeV.

$\theta_{c.m.}$ (in deg.)	$Q=0$ $d\sigma/d\Omega$	$Q=-0.845$ MeV $d\sigma/d\Omega$	$Q=-4.50$ MeV $d\sigma/d\Omega$
27.4	410	11.9	...
37.0	130	10.8	1.7
46.3	103	10.4	2.1
51.0	76.8	6.20	...
55.8	46.3	4.55	2.0
60.5	20.0	3.45	...
65.2	6.35	3.07	1.5
69.9	3.65	...	...
74.6	9.33	2.47	1.1
79.2	14.4	2.29	...
83.5	17.1	1.79	0.94
89.2	...	...	1.0
93.7	15.0	1.57	0.95
98.4	9.34	1.79	0.81
103.0	5.79	1.64	0.80
107.7	3.41	1.57	0.84
112.3	2.28	1.41	0.78
116.9	2.46	1.24	0.80
121.6	3.22	1.03	0.75
126.2	3.85	0.95	0.67
130.8	4.08	0.87	0.55
135.5	4.30	0.89	0.51
140.0	4.09	1.01	0.60
149.2	4.00	1.20	0.61
153.8	3.59	1.14	...
158.4	3.25	1.07	...
162.9	2.94	0.73	...
±0.1	±10% absolute	±10% absolute	±20% absolute

TABLE III. Differential cross sections for Ni$^{58}(p,p')$. The cross sections are in the center-of-mass system and have units of mb/sr. $E_p = 18.6$ MeV.

$\theta_{c.m.}$ (in deg.)	$Q=0$ $d\sigma/d\Omega$	$Q=-1.45$ MeV $d\sigma/d\Omega$	$Q=-4.5$ MeV $d\sigma/d\Omega$
27.4	322	7.74	...
36.9	115	8.41	1.4
46.3	83.2	5.57	2.5
55.7	39.3	2.80	1.5
60.5	20.5	2.07	1.5
65.1	6.02	1.74	1.1
69.9	3.25	1.79	0.93
74.6	5.83	1.94	0.87
79.2	11.5	1.87	1.2
83.9	14.2	1.65	0.92
88.5	15.0	1.65	0.92
93.2	12.3	1.30	0.94
97.9	9.19	0.96	0.94
102.5	5.40	0.87	0.70
107.2	3.19	0.80	0.78
111.9	2.26	0.66	0.70
116.4	2.31	0.62	0.64
121.1	2.80	0.48	0.54
125.7	3.16	0.47	0.50
130.3	3.68	0.52	0.58
134.9	3.92	0.59	0.56
139.5	4.17	0.77	0.61
144.1	4.23	0.84	0.63
148.8	4.11	0.86	0.56
157.9	3.60	0.83	
±0.1	$\pm10\%$ absolute	$\pm15\%$ absolute	$\pm25\%$ absolute

isotopes are also shown. The main interest in this work, the first 2$^+$ and 3$^-$ states in these isotopes, are so labeled in the figures. No angular distributions are reported other than for these states. It was of interest, however, to identify the various peaks and compare the determined Q values with known values. The well-known states in these nuclei are seen, and some less well-known or new states are identified. In Fe^{54}, a state or group of states at 6.4 MeV is seen. This is probably the same state seen in other scattering work.[2,23,24] In Fe^{56}, besides the known states a possible new state at 5.3-MeV excitation is seen. Evidence for this state has also been given by Wilson and Sampson in alpha scattering.[25] In Ni^{58}, few states are strongly excited by proton scattering, as evidenced by the figure. In Ni^{60}, besides the known states, a state (or states) at 5.2-MeV excitation is seen. In Ni^{62}, there is a suggestion of an excited state with energy $\sim$4.2 MeV, besides the well-known low-lying states and the 3$^-$ state at 3.80 MeV.

In Tables I–V are given the experimentally determined values of the absolute center-of-mass cross sections of the 2$^+$ and 3$^-$ states for the various isotopes. The accuracy of the center-of-mass angle is of the order of 0.1°, and the absolute errors in the cross sections are

[23] J. Bellicard and P. Barreau, Nucl. Phys. **36**, 476 (1962).
[24] M. Barloutaud et al., *Direct Interactions and Nuclear Reaction Mechanisms*, edited by E. Clementel and C. Villi (Gordon and Breach, Science Publishers, Inc., New York, 1962), p. 765.
[25] H. L. Wilson and M. B. Sampson, Phys. Rev. **137**, B305 (1965).

as given in the tables. Background subtractions and statistics were the limiting factors in the accuracy of the higher states. The relative errors, on the other hand, are estimated to be generally about 5% for the elastic cross sections, and 10% for the inelastic cross sections in most cases. In the case of Fe^{54}, the cross section for both the 4.81- and 6.40-MeV states are given, since it was not clear that the 4.81-MeV state was the corresponding 3$^-$ collective state so readily seen in the other isotopes. All incident energies were 18.6±0.05 MeV, except in the case of Fe^{56} where the scattering was examined at incident energies of 18.6 and 19.1 MeV. Within the accuracy of the experiment there was no difference between the cross sections at these two energies. Listed in Table II for Fe^{56} are the experimental results for an incident proton energy of 19.1±0.05 MeV. In the case of Ni^{60}, because of a wrinkle in the target and the subsequent uncertainty in target thickness, a somewhat arbitrary normalization of the cross-section data was made. After the nominal target thickness was included, all the data were normalized by a factor of 1.1. This was done to make the Ni^{60} data consistent with the Ni^{58} and Ni^{62} data, and was felt to be a safe procedure since such consistency has been shown in the data of Roberson and Funsten[7] at 17.5 MeV proton scattering. It was also impossible to achieve good optical-model fits to the elastic-scattering data for Ni^{60} without this normalization, while fits to the Ni^{58} and Ni^{62} data were fairly easily obtained.

TABLE IV. Differential cross sections for Ni$^{60}(p,p')$. The cross sections are in the center-of-mass system and have units of mb/sr. $E_p = 18.6$ MeV.

$\theta_{c.m.}$ (in deg.)	$Q=0$ $d\sigma/d\Omega$[a]	$Q=-1.33$ MeV $d\sigma/d\Omega$[a]	$Q=-4.08$ MeV $d\sigma/d\Omega$[a]
27.4	533	9.40	0.97
36.9	130	10.6	1.8
46.3	82.1	6.22	2.2
55.7	46.4	3.16	2.1
60.5	11.9	2.12	1.4
65.1	3.52	2.00	1.1
69.8	3.94	2.06	1.0
74.6	8.81	2.01	0.82
79.2	13.5	1.89	1.1
83.9	15.8	1.91	0.74
88.5	14.1	1.71	0.75
93.2	10.6	1.40	0.94
97.9	6.30	1.22	0.74
102.5	3.16	1.17	0.86
107.2	1.86	0.97	0.64
111.8	1.78	0.82	0.54
116.4	2.49	0.71	0.42
121.0	3.33	0.72	0.62
125.6	3.83	0.57	
130.2	3.95	0.62	
134.9	3.79	0.65	
139.4	3.58	0.82	
148.7	3.08	1.10	
157.9	3.01	1.04	
±0.1	$\pm10\%$ absolute	$\pm15\%$ absolute	$\pm25\%$ absolute

[a] Adjusted (see text).

TABLE V. Differential cross sections for $\text{Ni}^{62}(p,p')$. The cross sections are in the center-of-mass system and have units of mb/sr. $E_p = 18.6$ MeV.

$\theta_{c.m.}$ (deg.)	$Q=0$ $d\sigma/d\Omega$	$Q=-1.17$ MeV $d\sigma/d\Omega$	$Q=-3.80$ MeV $d\sigma/d\Omega$
27.3	467	9.83	⋯
36.9	154	10.72	2.2
46.3	84.2	6.14	2.9
55.7	27.0	3.39	2.0
60.4	9.96	2.54	1.9
65.1	3.49	2.42	1.4
69.8	5.93	2.10	⋯
74.5	12.2	2.14	1.1
79.1	17.4	2.14	0.94
83.9	17.6	1.72	0.97
88.5	15.3	1.66	0.94
93.2	10.7	1.48	0.96
102.5	2.40	1.10	0.80
107.1	1.45	0.971	0.78
111.8	2.20	0.727	0.66
116.4	3.21	0.714	0.70
121.1	4.23	0.564	0.63
125.6	4.52	0.563	0.51
130.2	4.43	0.565	0.59
139.4	3.33	0.709	0.38
148.7	3.23	1.10	0.33
153.0	3.11	1.12	⋯
157.9	3.13	0.975	⋯
±0.1	±10% absolute	±15% absolute	±25% absolute

Total cross sections for inelastic scattering to specific states were estimated by fitting the experimental points with a sum of Legendre polynomials, using a least-squares fitting routine. If $d\sigma/d\Omega = \sum_l a_l P_l(\cos\theta)$, then $\sigma = 4\pi a_0$. Sums of polynomials with from five to fifteen terms were used to fit the points, and the most reasonable fit was chosen to select the value of a_0. This usually came for twelve to thirteen polynomials in the sum for the 2^+ states, and about nine polynomials in the sum for the 3^- states. The values of a_0, the integrated inelastic cross sections, and typical total-absorption cross sections (found by an optical-model fit to the elastic cross-section data—see the next section) are given in Table VI. The accuracy of the integrated inelastic cross sections is felt to be about 10% for the 2^+ states and about 20% for the 3^- states, because of the uncertainty in the experimental points and the extrapolation of the fitted curves to 0° and 180°.

It should be noted how similar the three nickel isotopes are in the values of the integrated cross sections, with an increase as the mass number increases. The iron isotopes, on the other hand, are very different, the 2^+ state in Fe^{56} being about 2.5 times more highly excited than in Fe^{54}. If one looks at the tabular data in Tables I–V, it is seen that most of the difference is in the forward peaks, the ratio of peak heights being about 4 to 1. The 3^- states in all the isotopes except Fe^{54} have about the same integrated cross sections, and in the nickel isotopes are excited about one-third as strongly as the 2^+ states.

III. THEORETICAL FITS TO DATA

A. Elastic Scattering

In Fig. 2 are shown the elastic-scattering cross-section data fitted by optical-model calculations. The optical potential used was

$$U(r) = V_c(r) - Vf(r) - iWg(r) + V_s h(r)\boldsymbol{\sigma}\cdot\mathbf{l},$$

where the Coulomb part $V_c(r)$ is given by

$$V_c(r) = zz'e^2/r, \quad \text{for} \quad r \geq R_c$$
$$= zz'e^2/2R_c(3 - r^2/R_c^2), \quad \text{for} \quad r \leq R_c,$$

with $R_c = 1.25A^{1/3}$. The real part of the central potential $Vf(r)$ has a Saxon-Woods form factor

$$f(r) = [1 + \exp[(r-R)/a]]^{-1},$$

with a the diffuseness, and $R = R_c$. The imaginary part of the central potential $Wg(r)$ has a Gaussian form factor

$$g(r) = \exp[-(r - R_g)^2/b^2],$$

with $R_g = r_g A^{1/3}$ and $b = 0.60\Delta$, where $\Delta = $ full width at half-maximum of the Gaussian well. Finally the spin-orbit potential $V_s h(r)\boldsymbol{\sigma}\cdot\mathbf{l}$ has a form factor which is a derivative of the Saxon-Woods shape $f(r)$,

$$h(r) = (\hbar/m_\pi c)^2 \frac{1}{r}\frac{df(r)}{dr},$$

where $(\hbar/m_\pi c)^2 = 2.0$ F^2, and is the square of the Compton wavelength of the pion. The values of V, W, and V_s are then all positive numbers (potential depths) under the above definitions.

The optical model was applied in conjunction with an automatic search routine for finding optimum parameters, and was run on an IBM-7094 digital computer. The search routine minimized the quantity

$$\chi^2 = \sum_{i=1}^{N_d} \left[\frac{\sigma_i(\text{calc}) - \sigma_i(\text{expt})}{\Delta\sigma_i(\text{expt})} \right]^2,$$

where N_d is the number of experimental data points,

TABLE VI. Values of a_0 and $\sigma(\theta)$ from $\sigma(\theta) = \sum_l a_l P_l(\cos\theta)$, and total absorption cross section σ_{abs} for the various excited states in the Fe and Ni isotopes.

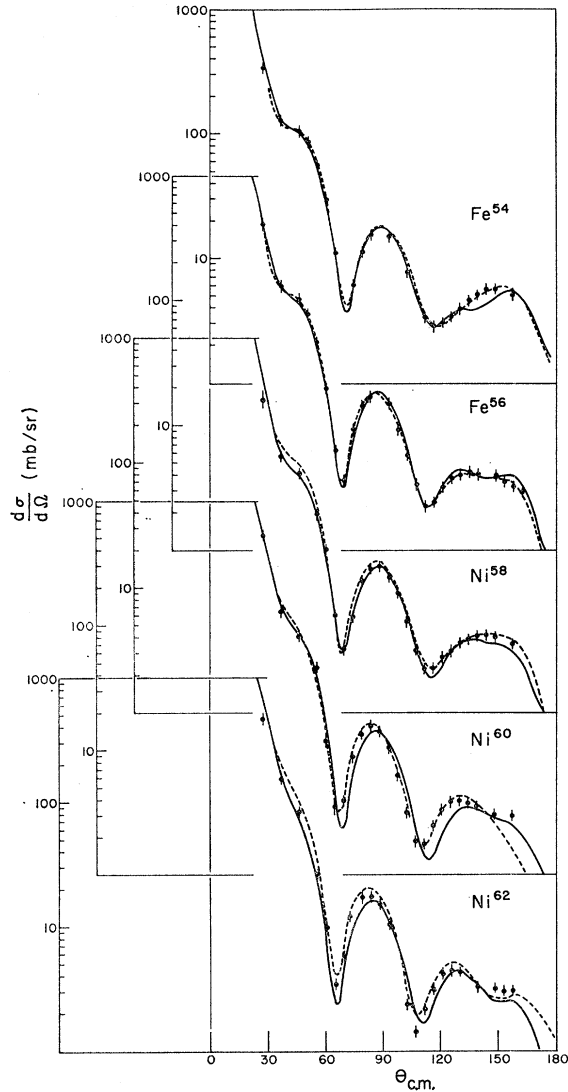|	J^π (E_{exc}, MeV)	σ_{abs} (mb)	a_0	$\sigma(\theta)$ (mb) inelastic
Fe^{54}	2^+(1.41)	974	1.52	19
	$(3^-, 4^+)$(4.81)		0.26	3.3
	(3^-)(6.40)		0.695	8.7
Fe^{56}	2^+(0.845)	990	3.71	47
	3^-(4.50)		1.01	13
Ni^{58}	2^+(1.45)	1040	2.45	31
	3^-(4.50)		0.90	11
Ni^{60}	2^+(1.33)	1084	2.84	36
	3^-(4.08)		0.85	11
Ni^{62}	2^+(1.17)	1106	2.92	37
	3^-(3.80)		1.02	13

FIG. 2. Differential cross-section data for elastic scattering of protons from Fe^{54}, Fe^{56}, Ni^{58}, Ni^{60}, and Ni^{62}. The curves are optical-model calculations, the solid line being from a three-parameter search and the dashed line from a five-parameter search over optical-model variables.

and $\Delta\sigma_i$(expt) is the standard deviation in each datum point. Two sets of searches were carried out. In one V, W, and a were allowed to vary in order to obtain a minimum in χ^2, while in the other set b and R_g were permitted to vary in addition to V, W, and a. The first set will be referred to as the three-parameter search and the second as the five-parameter search. The values of the parameters obtained as a result of these searches are given in Table VII. The quantity

$$S^2 = \chi^2/(N_d - N_p) ,$$

where N_d is the number of data points and N_p the number of parameters, gives an unbiased estimate of the quality of the fit and should be approximately equal to,

or less than, unity for a good fit. In Fig. 2 the solid lines are the optical-model fits obtained from the three-parameter searches, while the dashed curves are the results of the five-parameter searches.

Excellent fits are obtained for the Fe^{54} and Fe^{56} data. The quality of the fit deteriorates however from Ni^{58} to Ni^{62}. Inspection of the data reveals that the second minimum deepens and migrates towards smaller angles faster than the first minimum. The searches over three parameters are not able to fully account for this behavior, but with five parameters varying, this effect can be reproduced. The elastic-scattering part of a coupled-equation calculation (see next section) also reproduces the shifting of the minima.

B. Inelastic Scattering

The inelastic-scattering cross sections are assumed to be caused by a direct reaction, exciting either collective nuclear states or shell-model states.

1. Collective Excitations

The cross sections for collective excitations were calculated under the distorted-wave Born approximation,[26] with the differential cross section being given by

$$d\sigma/d\Omega = [M^2/(2\pi\hbar^2)^2](k_f/k_i)\,|A\,(\mathbf{k}_i,\mathbf{k}_f)|^2 ,$$

where M is the reduced mass of the system, $\mathbf{k}_i$ and $\mathbf{k}_f$ are the wave numbers of the incident and scattered particles, respectively, and $A\,(\mathbf{k}_i,\mathbf{k}_f)$ is the transition amplitude for the scattering process. The transition amplitude can be written as

$$A\,(\mathbf{k}_i,\mathbf{k}_f) = \langle\phi_f^{(-)}(\mathbf{k}_f)\,|\,V - \bar{V}\,|\,\phi_i^{(+)}(\mathbf{k}_i)\rangle ,$$

where V is the interaction between the two nuclei in the exit channel, and $\bar{V}$ is the optical potential in the exit channel. The ϕ are the distorted waves in the entrance and exit channels, and are found from fitting the elastic scattering with an optical model.

TABLE VII. Optical model parameters (energies in MeV, lengths in F) found from a three-parameter and a five-parameter search.[a] Also given are the number of data points, and values of χ^2 and S^2, measures of the goodness of fit.

Target	V	W	a	b	R_g	R	N_d	N_p	χ^2	S^2
Fe^{54}	47.7	10.9	0.702	1.00	4.72	4.72	22	3	32	1.7
	46.8	11.7	0.729	1.31	4.94	4.72	22	5	12	0.7
Fe^{56}	48.3	11.5	0.710	1.00	4.78	4.78	26	3	22	1.0
	47.4	11.9	0.778	1.30	4.97	4.78	26	5	4	0.2
Ni^{58}	47.5	13.0	0.808	1.00	4.84	4.84	25	3	55	2.5
	46.9	12.5	0.823	1.00	4.94	4.84	25	5	37	1.9
Ni^{60}	47.1	14.1	0.750	1.00	4.89	4.89	24	3	186	8.9
	47.7	16.7	0.856	0.92	5.30	4.89	24	5	41	2.2
Ni^{62}	49.6	13.4	0.748	1.00	4.95	4.95	23	3	147	7.4
	48.9	14.7	0.782	0.95	5.23	4.95	23	5	52	2.9

[a] N_d = number of data points. N_p = number of free parameters. $S^2 = \chi^2/(N_d - N_p)$ (should be $\lesssim 1$ for good fit). V_s = 7.00 MeV, and held constant.

[26] W. Tobocman, *Theory of Direct Nuclear Reactions* (Oxford University Press, New York, 1961).

A computer code called Direct Reaction Calculation (DRC),[27] was used for the calculation of the transition amplitudes and cross sections on the basis of the DWBA. The optical-model potentials used in the calculations were taken to be the values found from the three-parameter search to the elastic-scattering data (see Table VII). No significant differences were found for the magnitudes or shapes of the DWBA angular distributions using either the three-parameter or five-parameter potentials and geometries. Since the optical potentials are specified by the elastic scattering, the only free parameter in the inelastic-scattering fits to experiment is an over-all magnitude factor, which can be related to the deformation parameter β through the relation

$$(d\sigma/d\Omega)_{\text{expt}} = \beta^2 (d\sigma/d\Omega)_{\text{calc}}.$$

A quadrupole deformation of a nucleus can be written as

$$R(\theta') = R_0[1 + \beta_2 Y_2^0(\theta')],$$
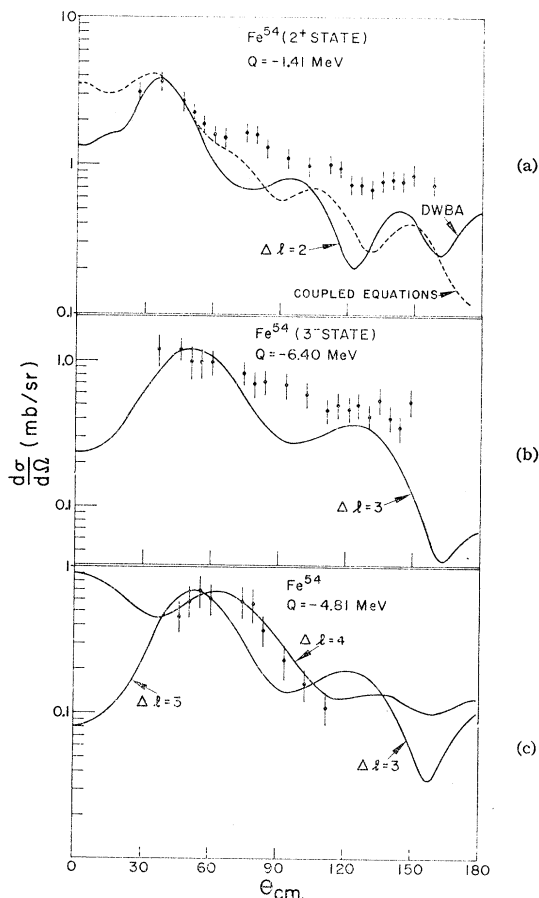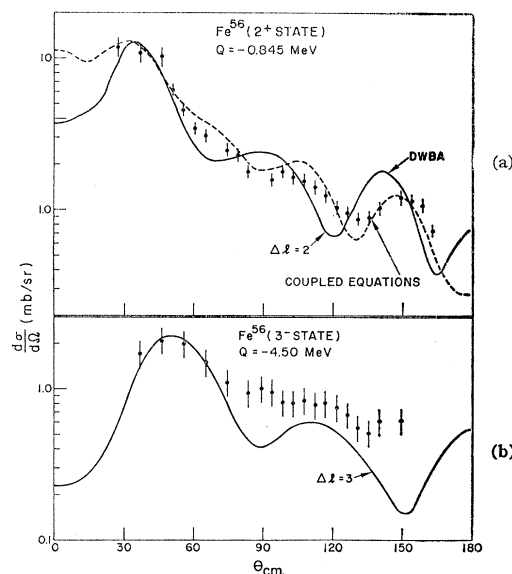
FIG. 3. Differential cross sections for inelastic proton scattering to states in Fe^{54}. The solid curves are DWBA calculations, while the dashed curves are the results of a coupled-equations calculation. (a) The 2⁺, 1.41-MeV excited state, (b) the 3⁻, 6.4-MeV excited state, and (c) the (3⁻ or 4⁺), 4.81-MeV excited state.

FIG. 4. Differential cross sections for inelastic proton scattering to states in Fe^{56}. The solid curves are DWBA calculations, while the dashed curves are the results of coupled-equations calculations (a) The 2⁺, 0.845-MeV excited state, and (b) the 3⁻ 4.50-MeV excited state.

where R is the radius of the nucleus. In a vibrational model, to first order, β is related to the restoring-force parameter C_l by

$$\beta_l^2 = (2l+1)\hbar\omega_l/2C_l.$$

The calculations using the code DRC do not distinguish between a rotational or vibrational excitation, in that only the value of β can be determined, and not whether this is associated with a permanently deformed nucleus, or a vibrational excitation.

The β_l can also be related to the reduced nuclear transition probability for an electric excitation of an excited state $B(El)$ through the following relation[28]

$$\frac{B(El)}{B(El)_{\text{sp}}} = \frac{(3+l)^2 Z^2}{4\pi(2l+1)}\beta_l^2$$

for a radiative transition of multipole order El. $B(El)_{\text{sp}}$ is the single particle unit.

In Figs. 3–7 are shown the fits of the experimental data and the calculated cross sections. They have been normalized at the forward peak, and the values of β_l extracted. The solid curves are the results of calculations using the potentials and geometry found from fitting the elastic scattering. The calculations also include Coulomb excitation as a possible mechanism. The fits of the DWBA calculations to the excited states of Fe^{54} are only fair. In the case of the 2⁺ state the forward peak is generally fit, but the curve misses the rest of the points badly. The fit for the 6.40 MeV state is also unsatisfactory. The calculations for the states in Fe^{56} fit

[27] W. R. Gibbs, V. A. Madsen, J. A. Miller, W. Tobocman, E. C. Cox, and L. Mowry, NASA Tech. Report TN D-2170, 1964.
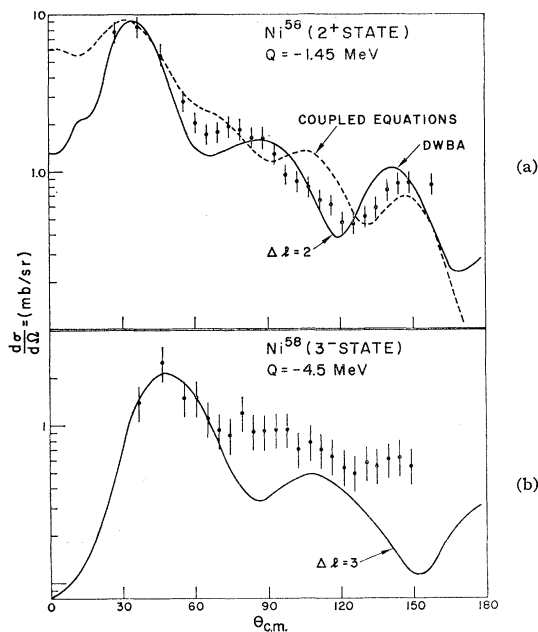
[28] K. Alder et al., Rev. Mod. Phys. 28, 432 (1956).

FIG. 5. Differential cross sections for inelastic proton scattering to states in Ni^{58}. The solid curves are DWBA calculations, while the dashed curves are the results of coupled-equations calculations. (a) The 2^+, 1.45-MeV excited state, and (b) the 3^-, 4.50-MeV excited state.

TABLE VIII. Deformation parameters determined by fitting calculations to experimental inelastic scattering.

		β_l^a	β_l^b	β_l^c	β_l^d	β_l^e
Fe^{54}	2^+	0.17	0.15	0.16	0.14	0.14
	(3^- or 4^+)	0.13	0.12	0.13	0.13	$\cdots$
	(3^-)	0.15	0.15	0.16	0.15	$\cdots$
Fe^{56}	2^+	0.31	0.28	0.28	0.25	0.24
	3^-	0.22	0.21	0.20	0.19	$\cdots$
Ni^{58}	2^+	0.24	0.22	0.24	0.21	0.21
	3^-	0.19	0.18	0.19	0.18	$\cdots$
Ni^{60}	2^+	0.28	0.25	0.30	0.26	0.26
	3^-	0.21	0.20	0.22	0.21	$\cdots$
Ni^{62}	2^+	0.30	0.27	0.27	0.25	0.23
	3^-	0.24	0.23	0.21	0.20	$\cdots$

[a] DWBA using "standard potential," including Coulomb excitation as possible mechanism.
[b] Same as (a) except no Coulomb excitation.
[c] DWBA using "best-fit potentials and geometry" including Coulomb excitation as possible mechanism.
[d] Same as (c) except no Coulomb excitation.
[e] Calculated with coupled-equations code, but no Coulomb excitation. Ground state coupled to first 2^+ and to second 2^+ state.

the data much better than for Fe^{54}. The 2^+ calculation gives the average behavior quite well, but does differ in detail. The 3^- state scattering is well fitted in the forward peak, but the data are higher at back angles. The fits of the calculations for the three nickel isotopes are very similar to those for the states in Fe^{56}, as can be seen in Figs. 5–7.

In the case of the 4.81-MeV state in Fe^{54}, a DWBA calculation was made for a change in angular momentum of both 3 and 4 units. This was done because it was not clear that this state, even though the energy was reasonable, was the corresponding 3^- vibrational state seen in Fe^{56} and in the nickel isotopes. As is seen in Fig. 3 the curve for $\Delta l=4$ fits well, while the $\Delta l=3$ curve is a poorer fit to the experimental data. While it is suggestive on the basis of these fits that the state has a spin and parity of 4^+, and not 3^-, it is not conclusive, and there still is an ambiguity in the spin and parity assignment.[29] It should be noted that alpha-particle scattering data[24,30] to this state is inconsistent with a spin-parity assignment of 3^-. What are needed in proton scattering are good small-angle data to resolve the question. Unfortunately, these data are not easy to obtain because of the large background subtraction necessary. The only other state in Fe^{54} which is excited with any intensity is the state of 6.40 MeV, and this state could be the collective vibrational state with $J^\pi=3^-$. Figure 3 also

shows a fit of a $\Delta l=3$ DWBA curve to the experimental data for this state.

The values of β, the deformation parameter, deduced from these fits of the DWBA calculations to the experimental points using the first peak as the normalizing criterion are shown in Table VIII. Also given in the table are values of β determined from a comparison of experiment and DWBA calculations using "standard potentials" as given by Perey.[18] These "standard potentials" are listed in Table IX. The fits to the experimental data are not better using Perey's parameters than with the parameters found from a detailed fit of the elastic scattering in each case.
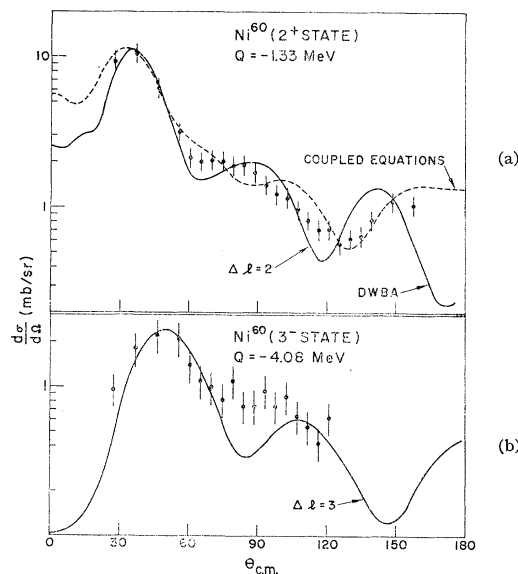
[29] J. S. Blair, Argonne National Laboratory Report No. ANL-6878, 1964, pp. 151–152 (unpublished).

[30] H. Faraggi and J. Saudinos, Argonne National Laboratory Report No. ANL-6848, 1964, p. 137 (unpublished).

FIG. 6. Differential cross sections for inelastic proton scattering to states in Ni^{60}. The solid curves are DWBA calculations, while the dashed curves are the results of coupled-equations calculations. (a) The 2^+, 1.33-MeV excited state, and (b) the 3^-, 4.08-MeV excited state.
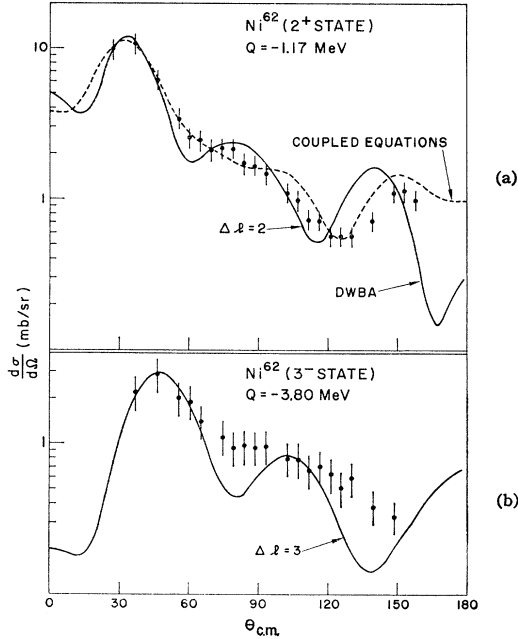
FIG. 7. Differential cross sections for inelastic proton scattering to states in Ni^{62}. The solid curves are DWBA calculations, while the dashed curves are the results of coupled-equations calculations. (a) The 2⁺, 1.17-MeV excited state, and (b) the 3⁻, 3.80-MeV excited state.

The inelastic-scattering angular distributions to the first 2⁺ state in each nucleus were also analyzed using the coupled-equations method, in which the 2⁺ state was described by the quadrupole vibrational model. A computer code written by Wills[31] was used for the computations. Previous computer studies[18] comparing optical-model, coupled-equations, and distorted-wave calculations in this mass and energy region permitted a modification of the potential obtained from the ordinary optical model. In the following expressions the primed terms are the parameters used in the coupled-equations calculation, and the unprimed terms are the parameters from the (five-parameter) optical-model search de-

TABLE IX. Standard potentials and geometry used in DWBA calculations.[a] (Units are MeV and fermis.)

	V	W	a	b	V_s[b]	R
Fe⁵⁴	46.9	10.0	0.65	1.00	6.50	4.72
Fe⁵⁶	47.4	11.6	0.65	1.00	6.50	4.78
Ni⁵⁸	46.9	9.9	0.65	1.00	6.50	4.84
Ni⁶⁰	47.8	11.4	0.65	1.00	6.50	4.89
Ni⁶²	48.5	12.8	0.65	1.00	6.50	4.95

[a] The same form factors as described earlier were used.
[b] V_s is taken to be zero in the code DRC. V and W were calculated by the formulas of Perey (Ref. 18):

$$V = 53.3 - 0.55E + [0.4ZA^{-1/3} + 27(N-Z)/A] \text{ MeV};$$

$$W = 8.2 + 48(N-Z)/A.$$

[31] J. G. Wills, Ph.D. thesis, University of Washington, 1963 (unpublished).

scribed in Sec. II:

$$V' = V - 14\beta_2^2,$$

$$W' = W - (25/b)\beta_2^2.$$

The computer program generates both elastic and inelastic cross sections. However, since it did not include spin-orbit distortions, the calculated elastic angular distributions had too deep minima and did not reproduce the extreme back angle data. It is expected that the addition of a spin-orbit interaction would give quite good fits to the elastic data. The positions of the minima, and their change from isotope to isotope, agree nicely with the experimental data.

The dashed curves in Figs. 3–7 are the results of the coupled-equations calculations. Except for the Fe⁵⁴ case the fits are reasonably good, and in some cases are an improvement over the distorted-wave Born approximation. It should be noted, however, that part of this improvement is most likely due to the fact that the coupled-equations code used a complex interaction, while DWBA used only a real interaction. Satchler et al. have shown[32,33] that a DWBA calculation with complex interaction can also give quite good fits. It is interesting to note that both the distorted-wave and the coupled-equations calculations give a ratio of the magnitude of the peak at 30 deg to that at 150 deg of approximately 10. In the case of Fe⁵⁴ this ratio is experimentally only 4. The shape of the forward maximum in the Fe⁵⁶ 2⁺ state angular distribution is qualitatively different from the corresponding curves in the Ni isotopes studied. This phenomenon is reproduced by the coupled-equation calculation, but not by the DWBA.

2. Particle-Model Excitations

Differential cross sections were also calculated using a particle model for the excitation of the first 2⁺ excited states of Fe⁵⁴ and Fe⁵⁶. For Fe⁵⁴ the ground and first excited states are both assumed to consist of a pure $(1f_{7/2})^{-2}$ configuration; in Fe⁵⁶ they are assumed to be pure $(1f_{7/2})^{-2}$, $(2p_{3/2})^2$. The object of these calculations was to determine to what extent a pure configuration calculation could produce the large ratio of cross sections for the excitation of the first 2⁺ state in Fe⁵⁶ to that in Fe⁵⁴. From Figs. 3 and 4, the ratio of the forward maximum of the differential cross sections is about 4 to 1. In the particle model, a larger cross section for Fe⁵⁶ is possible simply because there are four degrees of freedom compared to two in Fe⁵⁴.

The ground and first excited states of Fe⁵⁴ are uniquely determined by their angular momenta, but for Fe⁵⁶ there are two basis functions for the ground state and four for the first excited state.[34] The wave

[32] K. Yagi, H. Ejiri, M. Furukawa, Y. Ishizaki, M. Koike, K. Matsuda, Y. Nakajima, I. Nonaka, Y. Saji, E. Tanaka, and G. R. Satchler, Phys. Letters 10, 186 (1964).
[33] M. P. Fricke and G. R. Satchler, Phys. Rev. 139, B567 (1965).
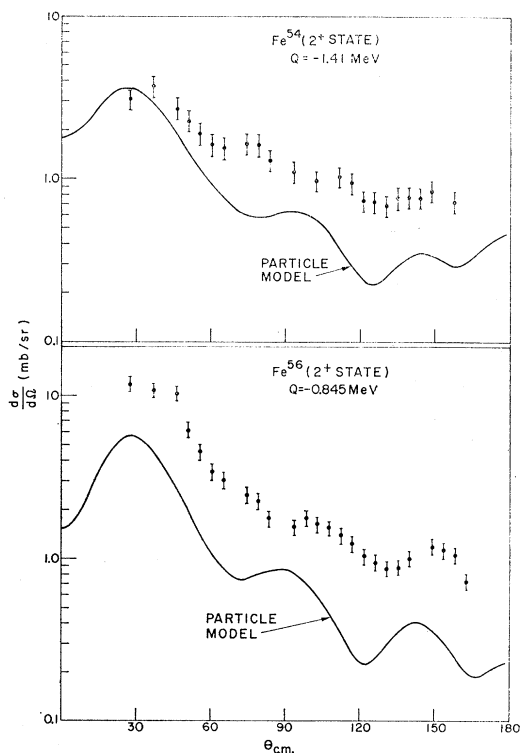[34] A similar type of analysis on Ar⁴⁰ has been carried out by S. Iwao, Nucl. Phys. 42, 46 (1963).

FIG. 8. Differential cross section for inelastic proton scattering to the first 2^+ excited state in Fe^{54} and Fe^{56}. The solid curve is the result of a particle-model calculation.

functions may be written

$$\psi_J^M = \sum_{J_N J_P} A_{JJ_P J_N} | JM (J_P(\tfrac{7}{2},\tfrac{7}{2}), J_N(\tfrac{3}{2},\tfrac{3}{2})) \rangle ,$$

where J_P is the angular momentum of the two proton holes and J_N is that of the two neutrons assumed to be in the $2p_{3/2}$ shell. The coefficients $A_{JJ_N J_P}$ are determined by diagonalizing the interaction Hamiltonian. Instead of diagonalization the following procedure was adopted for the Fe^{56} calculation. The two ground-state coefficients A_{022} and A_{000} were assumed to be known and the inelastic differential cross section was maximized with respect to the final-state coefficients. This gives a good estimate of the largest possible cross section which can be obtained from pure configurations in Fe^{56}. The wave function determined in this way is probably fairly close to being correct. In particular, the phases of the various terms are expected to be right, since the ground to first excited state transition tends to be one in which various single-particle transition terms interfere constructively,[16] leading to a large cross section. The maximization procedure will also lead to constructive interference.

Under these assumptions the Fe^{56} cross section is simply the sum of the cross sections for the $(1f_{7/2})^{-2}$, $0^+ \rightarrow 2^+$ transition and the $(2p_{3/2})^2$, $0^+ \rightarrow 2^+$ transition. In effect, all the 2^+ transition strength has been con-

centrated on the first of four possible pure configuration 2^+ states.

The particle model calculations were carried out using the computer code DRC with a Wigner interaction potential of a Yukawa form,

$$V(r) = V_0(e^{-\alpha r}/\alpha r) ,$$

between the projectile and the target nucleon. Parameters used were $\alpha = 0.7$ F^{-1}, and $V_0 = 48.4$ MeV. This range parameter α is near the meson theoretical value and along with V_0 fits the triplet effective range and scattering length. Exchange integrals are neglected. The results, compared to experiment, are shown in Fig. 8. The calculated ratio of the Fe^{56} to Fe^{54} absolute cross section at the first peak is 1.65, far short of the experimental ratio of 4 to 1. The calculated absolute cross section is close to experimental in Fe^{54} in agreement with the results of Funsten, Roberson, and Rost,[4] while in Fe^{56} it is much too small. It is probable that the pure $(1f_{7/2})^{-2}$ configuration describes fairly accurately the ground and first excited state of Fe^{54}, whereas the failure of the pure $(1f_{7/2})^{-2}(2p_{3/2})^2$ configuration for the Fe^{56} cross-section calculation indicates that a large amount of constructive configuration mixing is required. The first excited state of Fe^{56} is therefore expected to be strongly collective. This conclusion is in agreement with evidence[35] that Fe^{56} has a rotational spectrum.

IV. DISCUSSION

The nuclear optical model generally fits the experimental data well. In the case of the Fe isotopes the fits are extremely good, but are only fair for the Ni isotopes (see Table VII for a quantitative comparison of the fits). As was expected if more parameters are allowed to vary, the fits become better. The values of V and W generally increase with mass number within an element, and are close to those values found by Perey.[18] The increase in V can be accounted for by a nuclear symmetry term in the optical potential. The geometry factors, on the other hand, are quite different from those of Perey, the diffuseness for example being between 0.7 and 0.8 F, roughly 15% larger than the "standard" diffuseness.

The most important result, we feel, of these elastic-scattering fits, is the larger value of R_g, the center of the Gaussian absorption, compared to the "radius" of the Saxon-Woods potential. The values of the width b of the Gaussian absorption vary in a nonuniform manner, but the product of b, R_g, and W which is proportional to the "volume" of the Gaussian absorption is fairly constant, varying by about $\pm 10\%$ over the range of isotopes. The parameters found from these elastic-scattering fits were used in the DWBA calculations, which left only the value of the deformation parameter β as a free variable in the inelastic analysis.

[35] R. K. Gupta and R. C. Sood, Progr. Theoret. Phys. (Kyoto) **31**, 509 (1964).

The forward peak in both the 2^+ and 3^- inelastic scattering angular distributions for all the isotopes is reasonably fit by the DWBA calculations, assuming a collective excitation. However the remainder of the angular distributions are not well reproduced. The integrated cross sections for the Fe^{56} data agree reasonably well with the calculation, but for the nickel isotopes the calculations give too small a value, the differential cross sections falling below the experimental data in the back angles.

The coupled-equations calculations, which included the ground state and the first and second 2^+ states, give reasonably good agreement with the experimental 2^+ differential cross-section data. Perey and Satchler[19] have shown that for values of β typically found for the iron and nickel isotopes, the DWBA and coupled-equations method are equivalent if applied consistently. The coupled-equations and DWBA calculations shown in the figures are not equivalent, however, since the DWBA contained only a real interaction potential, while the coupled-equations calculation had both a real and an imaginary interaction potential. Neither had a spin-orbit interaction, but both used surface absorption. Volume absorption was also tried but gave poorer fits to the data.

The coupled-equations calculations give better fits than do the DWBA in most cases, but the improvement is probably due to the inclusion of the imaginary interaction potential. Recently Fricke and Satchler[33] have shown that for 40-MeV proton scattering on Fe and Ni isotopes the DWBA and coupled-equations methods, both with a complex interaction potential, give the same results. It would be of interest to determine whether the same is true at 19 MeV.

Iron-54 seems to be a special case. The forward peak position is reasonably well fit, but the calculation curve past 60° (c.m.) is low by roughly a factor of 2. This is true in both the DWBA and coupled-equations calculations.

In the case of the particle model, even the forward peak is not well fit. The calculation gives an angular distribution very similar to those of the collective model, but the forward maximum occurs at too small an angle. This feature seems to be characteristic of the particle-model calculations using a Yukawa interaction[16, 36] and is due to the slow decrease of the interaction form factor at large r compared to the derivative Saxon-Woods

form given by the vibrational model. The effective nucleon-nucleon interaction in the inelastic-scattering process appears from this result to have a shorter range than the free nucleon-nucleon interaction. This conclusion must be regarded as tentative, since exchange effects have not yet been included.

The 3^- state seen easily in Fe^{56} and in the nickel isotopes is ambiguous in Fe^{54}. The evidence from this work seems to favor the state at 6.40 MeV as the collective 3^- state, but it is not conclusive. The collective state could appear at an excitation of about 4.8 MeV, but with the energy resolution inherent in this work other states would be included in the cross-section determination. This would change the apparent magnitude and angular variation of the cross section and thus diminish the agreement with theoretical calculations. The position of the 3^- collective state in Fe^{54} still is in question.

There have been many comparisons of β_l values determined from scattering experiments using different bombarding particles at various energies, and from Coulomb excitation measurements. For example, there are recent tabulations by Stovall and Hintz[2] and by Faraggi and Saudinos.[30] The accuracy of the scattering determinations of β_l depends on the absolute accuracy of the differential cross-section measurements. Typically the determination of β_2 is good to only about 7–10%, and for β_3 to about 10–15%. Different assumptions made in calculations of the differential cross sections, or ambiguities in the parameters chosen for the calculations, also affect the values of β_l. This is clearly seen in Table VIII.

Therefore, any comparisons made among β_l values should take into consideration the above uncertainties in experiment, and the assumptions made in the calculations. Our values are in good agreement with other scattering determinations and with Coulomb excitation determinations. The values of β_2 for the nickel isotopes are somewhat larger than other estimates, but in view of the possible variations in β_l, we feel that this is not very significant.

ACKNOWLEDGMENTS

[36] V. A. Madsen, S. F. Eccles, and H. F. Lutz, Bull. Am. Phys. Soc. **9**, 724 (1964).